View metadata, citation and similar papers at core.ac.uk
brought to you by CORE
provided by Crossref

Single-particle spectroscopy of rare isotope beams: Calculations beyond the eikonal approximation

J.A. Tostevin*, D. Bazin†, B.A. Brown†, T. Glasmacher†, P.G. Hansen†, V. Maddalena†, A. Navin†[1] and B.M. Sherrill†

*Department of Physics, University of Surrey, Guildford, Surrey, GU2 7XH U.K.
†National Superconducting Cyclotron Laboratory, Michigan State University, East Lansing, Michigan 48824

Abstract. The momentum distributions of the residual nuclei after one-neutron removal, measured in coincidence with gamma rays, identify the excited levels of these residues. The resulting differential partial cross sections map the momentum content and structure of the removed-nucleon wave function and provide an exacting test of theory. Data for population of the ^{14}C and ^{10}Be ground states show an asymmetry that is incompatible with the currently used eikonal descriptions. A fully dynamical description of the elastic breakup mechanism provides an understanding of the new observation, which will be most pronounced for nuclear halo states. This interpretation is clarified by an analysis of the angular distribution of the heavy residues.

The ground state of ^{11}Be has a well-developed neutron halo with a neutron separation energy S_n of 0.503 MeV and a wave function dominated by a $1s_{1/2}$ neutron single-particle component. A recent experiment by Aumann *et al.* [1] studied the ^{9}Be(^{11}Be,^{10}Be+γ)X one-neutron removal reaction at 60 MeV/nucleon, applying a subtraction procedure to construct the cross section for events without a photon in coincidence. Significantly, the resulting parallel-momentum distribution of this ground-state to ground-state cross section, $d\sigma/dp_{||}$, shows a marked asymmetry that is incompatible with the assumptions of the eikonal theory used, and that the interpretation is incomplete.

In this paper an understanding of the observed asymmetry is provided by a fully dynamical description of the elastic breakup component of the cross section. The empirical findings for ^{11}Be are also confirmed in a precise experiment on ^{15}C, with S_n=1.218 MeV. The dependence of the $d\sigma/dp_{||}$ distributions on the angle of the emerging core particle is shown to provide an additional insight and diagnostic of the reaction mechanism.

These results have significance beyond halo states. One-nucleon-removal reactions, applied to secondary beams produced from fragmentation, show promise as an effective tool for study of the evolution of single-particle states in rare nuclei [1, 2, 3, 4, 5, 6]. The partial cross sections to individual final states, measured by observing the photons from their in-flight decays, and their $d\sigma/dp_{||}$, identify both the orbital angular momenta of the removed nucleons and their spectroscopic factors. A recent systematic study of many *psd*-shell nuclei, but where the core states were not identified, adds further support to the power of the technique [7].

In the present experiment a radioactive beam of ^{15}C was produced by fragmentation of an 80 MeV/nucleon ^{22}Ne primary beam on a thick ^{9}Be target. The secondary beam was purified in the A1200 fragment separator and delivered through a dispersion-matching beam line to a 228 mg/cm^2 ^{9}Be target. The mid-plane energy was 54 MeV/nucleon. The target was surrounded by an array of NaI(Tl) gamma detectors operated in coincidence with the ^{14}C residues. These were detected in the S800 spectrograph, operated at a momentum resolution of 0.025%. After Doppler correction to the center-of-mass system, the three gamma rays (0.81, 6.09 and 7.01 MeV) could be identified as connecting known states in ^{14}C [8]. The energies, spin-parity assignments and l values are given in Table 1. The absolute intensities of the gamma rays combine with the measured inclusive cross section to give the partial cross sections, of which approximately 20% connect to excited levels. Details of the experimental techniques are given in [6].

[1] Permanent Address: Nuclear Physics Division, BARC, Trombay, Mumbai 400 085, India.

TABLE 1. Cross sections (in mb) and spectroscopic factors for the reaction ^{9}Be(^{15}C,^{14}C(I^{π}))X at $E = 54$ MeV/nucleon. The ^{15}C ground-state spin is $J^{\pi} = \frac{1}{2}^{+}$.

$E[MeV]$	I^{π}	l	σ_{sp}*	σ_{exp}	C^2S_{exp}	C^2S_{th}
0.00	0^+	0	147	109±13	0.74±0.09	0.98
6.094	1^-	1	31†	22±3	0.72±0.10	1.18
6.903	0^-	1	29†	3±1	0.10±0.03	0.46
7.102	2^+	2	30†	3±1	0.10±0.03	0.02
			σ_{tot}	137±16		

* Cross sections from the eikonal theory of Ref. [6]
† Calculated assuming a ^{13}C+n($1s$) composite core [3].

At fragmentation beam energies, $\approx$ 50MeV/nucleon and greater, theoretical analyses have, almost universally, exploited sudden and eikonal-like approximations. These lead to considerable practical simplifications and to calculation schemes with relatively simple and transparent physical inputs. They have been very successful [9, 10, 11, 12], with good agreement between different models. The eikonal reaction theory of Refs. [3, 6] was used to calculate the single-particle removal cross sections σ_{sp} and the resulting experimental spectroscopic factors shown in Table 1. The latter are in acceptable agreement with the theoretical values from the WBP interaction [13].

The shapes of the $d\sigma/dp_{||}$ are shown in Fig. 1. Eikonal estimates are also shown, based on profile functions with sharp cutoff radii chosen to reproduce the free neutron- and core-target reaction cross sections. The distribution to the 6.09 MeV 1^- level agrees well with the eikonal calculation (dot-dashed curve). That to the ground-state, however, shows an increased width and excess of intensity at low momenta when compared to the eikonal theory (dashed curve), as was seen for ^{11}Be [1]. These first indications of a systematic deficiency in the eikonal theory are evident because of the exclusive character and quality of the data shown in Fig. 1 and Ref. [1]. The ^{11}Be data are not shown, however, the measured ^{11}Be and ^{15}C ground state distributions, and their asymmetries, are essentially identical if their widths are divided by the bound-neutron asymptotic wave numbers computed from their separation energy. This scaling is what the sudden approximation would predict if the bound s-states were approximated by Yukawa wave functions.

The data shown in Fig. 1 are the sum of two distinct reaction mechanisms. The first, stripping, involves the removed

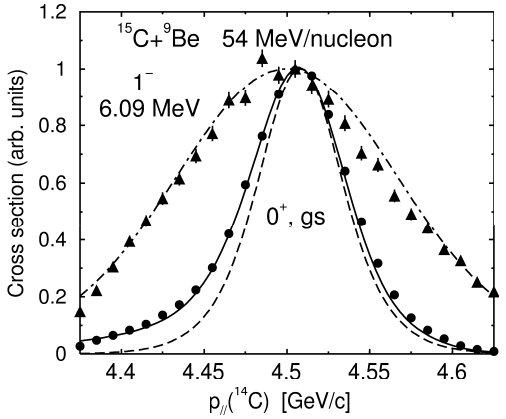

FIGURE 1. Distributions with the parallel momentum $p_{||}$ of the cross section to the ground state of ^{14}C (circles) and in coincidence with the 6.094 MeV gamma ray (triangles). (The latter contains a 10% contribution from feeding via the 6.90 MeV level. Coincidences with the 0.81 MeV gamma ray show this contribution, within the experimental errors, has the same l=1 shape.) Acceptance corrections are discussed in Ref. [6]. They amount to a factor 2 at the edges of the diagram. The dashed (gs) and dot-dashed (1^-) curves are the results of the eikonal-model calculations with the peak heights and positions adjusted to the data. (The theoretical 1^- peak has been centered 0.008 GeV/c lower than that of the ground state. The calibration was not precise enough to permit a discussion of the absolute position of the peaks relative to beam velocity.) The solid curve is the result of the CDCC analysis discussed in the text.

nucleon being absorbed by the target and hence being removed from the forward-going beam. The second, diffraction dissociation or elastic breakup, describes the separation of the neutron from the core by the neutron- and core-target tidal forces, the target remaining in its ground state. A characteristic of these reactions is their surface dominance, as evident from the fact that (1) the calculated stripping cross sections are much smaller than the free-neutron reaction cross sections, $\approx$ 300 mb, and (2) the momentum components associated with the inner part of the neutron wave function are absent from the ground state momentum distribution in Fig. 1 [14]. In Table 1 the sum of the cross sections from these single particle removal mechanisms are shown, calculated using the eikonal model of [6].

In Fig. 1 it has been assumed, as is usual [15], that the stripping and diffractive cross section components have the same shape. While the eikonal calculation (dashed line) clearly identifies the ^{14}C(gs) distribution as due to s-state nucleon removal its failure in detail is apparent. The width of the calculated eikonal distribution has been shown to retain a small sensitivity to the details of the profile functions used [16] and is not the issue. Our concern is the observed asymmetry. The sudden/eikonal approximations are implicitly energy non-conserving. The calculations do not treat energy sharing between the center of mass and relative motion degrees of freedom of the neutron and core or the deflection of the core from its assumed (eikonal) straight line path. A result is that the calculated distributions must be symmetric about the momentum corresponding to the beam velocity. That the asymmetry is pronounced for the halo states suggests that the phenomenon is associated with the elastic breakup mechanism and that there is a need to go beyond the eikonal theory.

In the present work, we develop the fully-quantum-mechanical coupled discretised continuum channels (CDCC) method [17] for the elastic breakup of ^{15}C and ^{11}Be. The CDCC treatment of breakup couples the incident projectile in spin state (I,M), in all orders, to breakup configurations (I',M') of the core and neutron, with spins (c,μ), (s,σ) and relative orbital angular momentum ℓ. That is, $\vec{I'}=\vec{j}+\vec{c}$ with $\vec{j}=\vec{\ell}+\vec{s}$. This continuum of breakup states, in each significant spin-parity excitation I', is further grouped into a number $\mathcal{N}$ of representative energy intervals or bins. In each bin i, with wavenumbers $[k_{i-1}\rightarrow k_i]$, a square integrable bin state $\hat{\phi}_\alpha, \alpha\equiv(i,(\ell s)jcI')$ is constructed [18] as a superposition of the scattering states in that interval. In the present applications, orbital angular momenta $\ell\leq$5 are needed for converged results and, in each I' channel, $\mathcal{N}$=10 bins were needed with energies from zero to 20 MeV in equal relative wavenumber intervals.

Each such bin state acts as an effective discrete excited state of the core+nucleon system. The solution of the Schrödinger equation in this model space is then carried out by partial wave expansion and the solution of the resulting coupled equations [20], generating a set of (two-body) inelastic transition amplitudes $T_{M'M}(\alpha,\vec{K}'_\alpha)$ for exciting each bin α, with center of mass wavenumber $\vec{K}'_\alpha$. The physical breakup amplitudes, to a given relative motion final state $\phi^{(+)}_{\mu\sigma}(c,\vec{k})$ of the core and nucleon are of the form [18]

$$T_{\mu\sigma;M}(\vec{k},\vec{K'}) = \frac{(2\pi)^{\frac{3}{2}}}{k}\sum_{\alpha\nu}(-i)^\ell\,(\ell\nu s\sigma|jm)\,(jmc\mu|I'M')\exp[i\delta_\alpha(k)]Y_{\ell\nu}(\hat{k})\;T_{M'M}(\alpha,\vec{K'})\;\;. \qquad (1)$$

Here $\delta_\alpha(k)$ is the neutron-core relative motion phase shift in excitation state I', the $T_{M'M}(\alpha,\vec{K'})$ are interpolated from the values calculated at the wavenumbers $\vec{K}'_\alpha$, and the sum is taken over all bins α which contain k. Hence the laboratory frame triple differential cross sections for the neutron and core fragments are obtained and, following integration over all directions of the unobserved neutron, and over any angular acceptance and the perpendicular momentum components of the heavy residue, the $d\sigma/dp_{||}$ differential cross sections.

The details of the calculations are as follows. The radial wave functions used to obtain the spectroscopic factors were obtained with a standard Woods-Saxon potential shape (r=1.25,a=0.7) which we have used consistently in the analysis of all knockout data in this region[6]. The absolute spectroscopic factors depend on the overlap function, for example, using a $s_{1/2}$ radial wave function obtained the SKX[19] Hartree-Fock calculation for ^{14}C would give C^2S_{exp}=0.90 for the ground state, but the shape of the momentum distribution is insensitive to the radial wave function. The depth of the binding potential is adjusted to reproduce the physical separation energy of the nucleon in the projectile ground state. The same interactions are used to construct the bin wave functions, except that the interaction in d-waves (p-waves) in the ^{15}C (^{11}Be) case is re-adjusted to correctly bind the known $d_{5/2}$ ($p_{1/2}$) state. This bound excited state is included as an additional coupled channel. The core-target interaction is calculated from the effective Gaussian nucleon-nucleon interaction of [3] and Gaussian matter distributions for the core and target. We assume root mean squared mass radii of 2.30, 2.28, 2.28, 2.36 fm for ^{14,13}C and ^{10,9}Be. A realistic description of the refractive content of the neutron-target optical potential is essential for a quantitative study of the relative contributions from the stripping and elastic breakup mechanisms [21]. In the coupled-channels calculations this is calculated from the same target density but using the mid-point local density approximation [22] and the Jeukenne, Lejeunne and Mahaux (JLM) [23] microscopic effective

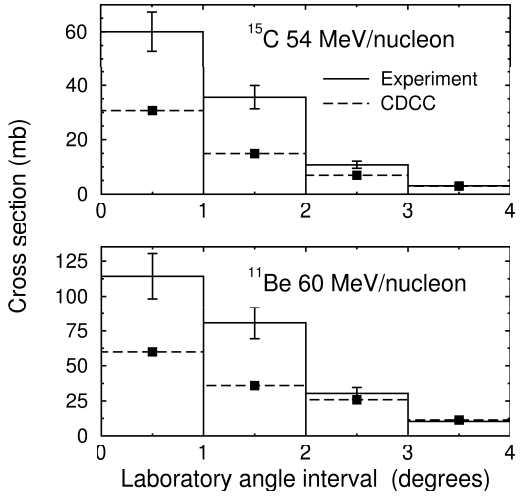

FIGURE 2. Measured partial cross sections (solid lines) for population of the ^{14}C(gs) (upper) and ^{10}Be(gs) (lower) in the laboratory angle intervals indicated, from the ^{15}C+^{9}Be and ^{11}Be+^{9}Be reactions at 54 and 60 MeV/nucleon, respectively. Since the experiments did not use tracking of the incoming projectiles, the (rms) resolution on the deflection angle was only 0.43°. The bin size of one degree here and in Fig. 3 has been chosen to avoid contributions of the resolution in the comparison. The CDCC elastic breakup calculations are shown by the dashed lines and filled squares.

nucleon-nucleon interaction. We apply the conventional scalings, 1.0 and 0.8, to the real and imaginary strengths [22]. To compare with the CDCC, eikonal calculations are repeated with the profile functions calculated from the same core- and neutron-target interactions using the exact continued phases method of reference [24].

The calculated diffraction dissociation $d\sigma/dp_{\|}$ from the CDCC show an asymmetry which becomes increasingly pronounced with increasing angle of acceptance of the detected core fragments. To clarify this phenomenon we calculate the differential cross sections for core fragments emerging in the laboratory angle intervals 0–1, 1–2, 2–3, and 3–4 degrees about the beam direction. The experimental partial cross sections to these angle bins are shown by the solid histograms in Fig. 2, for both the ^{15}C (upper) and ^{11}Be (lower) cases. The corresponding $d\sigma/dp_{\|}d\Omega$ of the ^{14}C(gs) are shown by the solid symbols in Fig. 3, which show clearly a broadening of the distributions and a shift in the peak position toward lower momenta with increasing scattering angle. The data in Fig. 3 sum to that shown in Fig. 1 for the full experimental acceptance.

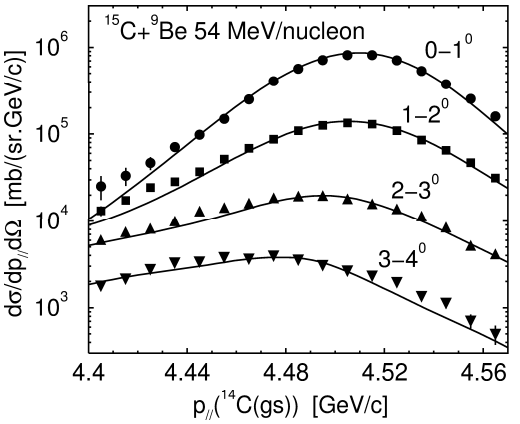

FIGURE 3. Measured differential parallel momentum distributions (solid symbols) of the ^{14}C(gs) in each of the laboratory angle intervals indicated, from the ^{15}C+^{9}Be reaction at 54 MeV/nucleon. The solid curves are the CDCC elastic breakup calculations supplemented, in the case of the upper three intervals, by the stripping cross section contributions required in Figure 2.

Evident from Fig. 2 is the generic nature of the ^{15}C and ^{11}Be results, differences being essentially in magnitudes, driven by the neutron separation energies in the two cases. Thus, for the $p_{\|}$ distributions, only the results for ^{15}C are discussed here. The calculated diffractive components of the cross section from the CDCC in each angle interval are shown by the dashed histograms and filled squares in Fig. 2. The total calculated elastic breakup cross section from the CDCC (with unit spectroscopic factor) is 55.6 mb. This is in excellent agreement with the eikonal values of 56 mb (for the calculation of Table 1) and of 67 mb when using the JLM neutron interaction. The latter calculates σ_{sp}=130 mb.

We note that theory predicts that the measured cross sections for residues emerging at angles greater than 2° are dominated by elastic breakup events. The stripping contributions, obtained as a difference, and the CDCC predictions are approximately equal at more forward angles, a long standing expectation from eikonal model calculations for the energies involved here [11]. We can therefore compare the largest angle CDCC calculations directly with the data in Fig. 3, assuming they arise from the diffraction dissociation mechanism only, the lower solid line. For the three smaller angle intervals we must add the appropriate cross section contribution due to stripping. The shape of the $p_{\|}$ distribution for these stripping contributions, as a function of core angle, is not known. In Fig. 3 these have been assumed to have the same shape as those from the CDCC calculation, which correctly takes into account energy and momentum conservation in the deflection of the core fragment. Using instead the $p_{\|}$ distribution shape from the eikonal calculation, shown in Fig. 1, produces a rather similar result, although it is inferior in detail. The solid curves in Fig. 3 sum to the solid curve in Fig. 1 for the full angle acceptance, providing an excellent description of the measured asymmetry and width of the distribution.

While the physical effects discussed are most pronounced for halo states, it will be important to take these deviations from eikonal theory into account in transitions that require an accurate adjustment to mixed l=0,2 momentum profiles, such as were seen in [5, 6]. Furthermore, the present analysis establishes that the reaction mechanisms in nucleon removal reactions can be understood in detail and accurately described. This is an essential step in their use for mapping single-particle strength and the evaluation of structure theories in hitherto inaccessible regions.

ACKNOWLEDGMENTS

This work was supported by EPSRC(UK) Grant No. GR/M82141 and by NSF Grants No. PHY 9528844 and No. PHY 0070911. The advice of Ian Thompson on the use of FRESCO is gratefully acknowledged.

REFERENCES

1. Aumann, T., *et al.*, Phys. Rev. Lett. 84, 35 (2000).
2. Navin, A., *et al.*, Phys. Rev. Lett. 81, 5089 (1998).
3. Tostevin, J.A., J. Phys. G 25, 735 (1999).
4. Navin, A., *et al.*, Phys. Rev. Lett. 85, 266 (2000).
5. Guimarães, V., *et al.*, Phys. Rev. C 61, 064609 (2000).
6. Maddalena, V., *et al.*, Phys. Rev. C 63, 024613 (2001).
7. Sauvan, E., *et al.*, Phys. Lett. B 491, 1 (2000).
8. Ajzenberg-Selove, F., Nucl. Phys. A523, 1 (1991).
9. Yabana, K., Ogawa Y., and Suzuki, Y., Phys. Rev. C 45, 2909 (1992); Nucl. Phys. A539, 295 (1992).
10. Al-Khalili, J.S., Thompson, I.J., and Tostevin, J.A., Nucl. Phys. A581, 331 (1995).
11. Hencken, K., Bertsch, G., and Esbensen, H., Phys. Rev. C 54, 3043 (1996).
12. Bonaccorso, A., and Brink, D.M., Phys. Rev. C 58, 2864 (1998).
13. Warburton, E.K., and Brown, B.A., Phys. Rev. C 46, 923 (1992).
14. Hansen, P.G., Phys. Rev. Lett. 77, 1016 (1996).
15. Barranco, F., and Vigezzi, E., *International School of Heavy-Ion Physics, 4th Course: Exotic Nuclei*, ed. by R.A. Broglia and P.G. Hansen (World Scientific, Singapore, 1998) p217.
16. Parfenova, Yu.L., Zhukov, M.V., and Vaagen, J.S., Phys. Rev. C 62, 044602 (2000).
17. Kamimura, M., *et al.*, Prog. Theor. Phys. Suppl. 89, 1 (1986); Austern, N., *et al.*, Phys. Rep. 154, 125 (1987).
18. Tostevin, J.A., Nunes, F.M., and Thompson, I.J., Phys. Rev. C 63, 024617 (2001).
19. Brown, B.A., Phys. Rev. C 58, 220 (1998).
20. Thompson, I.J., Comp. Phys. Rep. 7, 167 (1988); FRESCO users' manual, University of Surrey, UK.
21. Tostevin, J.A., Nucl. Phys. A682, 320c (2001).
22. Petler, J.S., Islam, M.S., Finlay, R.W., and Dietrich, F.S., Phys. Rev. C 32, 673 (1985).

23. Jeukenne, J.-P., Lejeune, A., and Mahaux, C., Phys. Rev. C 16, 80 (1977).
24. Brooke, J.M., Al-Khalili, J.S., and Tostevin, J.A., Phys. Rev. C 59, 1560 (1999).